

# **Extending application limits of scaling relations for time-resolved Monte Carlo simulations in diffuse optics**

## **Citation:**

Lorenzo Spinelli, Andrea Farina, Antonio Pifferi, Alessandro Torricelli, Angelo Sassaroli, Fabrizio Martelli, "Extending application limits of scaling relations for time-resolved Monte Carlo simulations in diffuse optics," Proc. SPIE 13314, Optical Tomography and Spectroscopy of Tissue XVI, 1331404 (20 March 2025); <https://doi.org/10.1117/12.3042911>

## **Copyright notice:**

Copyright 2025 Society of Photo-Optical Instrumentation Engineers. One print or electronic copy may be made for personal use only. Systematic reproduction and distribution, duplication of any material in this paper for a fee or for commercial purposes, or modification of the content of the paper are prohibited.

## **DOI abstract link:**

<https://doi.org/10.1117/12.3042911>

# Extending application limits of scaling relations for time-resolved Monte Carlo simulations in diffuse optics

Lorenzo Spinelli<sup>a</sup>, Andrea Farina<sup>a</sup>, Antonio Pifferi<sup>a,b</sup>, Alessandro Torricelli<sup>a,b</sup>, Angelo Sassaroli<sup>c</sup>, and Fabrizio Martelli<sup>d</sup>

<sup>a</sup>Istituto di Fotonica e Nanotecnologie, CNR, Piazza Leonardo da Vinci 32, Milano, 20133, Italy

<sup>b</sup>Dipartimento di Fisica, Politecnico di Milano, Piazza Leonardo da Vinci 32, Milano, 20133, Italy

<sup>c</sup>Department of Biomedical Engineering, Tufts University, 4 Colby Street, Medford, Massachusetts, 02155, USA

<sup>d</sup>Dipartimento di Fisica e Astronomia, Università degli Studi di Firenze, Via Giovanni Sansone 1, Sesto Fiorentino, 50019, Italy

## ABSTRACT

An analytic approximation of the distribution functions of scattering events occurring during photon migration in scattering media is proposed. This allows extending the range of applicability of scaling relations for scattering coefficient to generate new simulations starting from an existing Monte Carlo simulation. Time Point Spread Functions for a uniform variation in the scattering coefficient up to  $\pm 50\%$  are calculated by using the analytic approximation of the scattering event distribution functions and compared with the exact Monte Carlo simulations: the largest deviations from time point spread functions directly obtained by Monte Carlo simulations occur for late arrival times and are  $\lesssim 50\%$ .

**Keywords:** Scaling relations, Light propagation in scattering media, Monte Carlo simulations, Scattering coefficient

## 1. INTRODUCTION

The execution of reliable Monte Carlo (MC) simulations to numerically describe photon migration in diffusive media is in many cases limited by the overwhelming computational time, even if the advancement in computational power offered by graphic processing units (GPUs) is recently exploited in MC tools.<sup>1,2</sup> The possibility to use scaling relations (SR) to MC simulations is, then, a great advantage.<sup>3</sup> As a matter of fact, SR are already widespread used as an efficient way to take into account properties of the medium absorption properties, by using the microscopic Lambert-Beer law. On the contrary, the scaling approach applied to the scattering coefficient is more critical.<sup>4</sup> As shown in two recent papers,<sup>5,6</sup> the scaling of the scattering coefficient  $\mu_s$  leads to convergence problems, mainly due to the dependence of the scaling factor on the number of scattering events  $k$  each photon experiences during its travel through the diffuse medium.

In this work we want to study the statistics of the scattering events in photon migration, by evidencing a key feature of the probability function  $p_\ell(k, \mu_s)$  for the number of scattering events  $k$  undergone by a detected photon along a path of length  $\ell$ , that will allow to apply the scaling of the scattering coefficient for a wider range of values than that found in Ref. 6.

## 2. STATISTICS OF SCATTERING EVENTS IN HOMOGENEOUS DIFFUSE MEDIA

From a MC simulation, we can reconstruct the Time Point Spread Function (*TPSF*) by classifying the weights of the received photons into a histogram of their time-of-flight  $t$ . Due to the presence of the number  $k$  of scattering interactions in the SR for the scattering coefficient, a straightforward calculation of the  $TPSF(\mu_s, t)$  for a varied  $\mu_s$  starting from the

---

Send correspondence to Lorenzo Spinelli: e-mail: [lorenzo.spinelli@polimi.it](mailto:lorenzo.spinelli@polimi.it)

$TPSF(\mu_{s0}, t)$  for an initial  $\mu_{s0}$  is possible once the probability function  $p_\ell(k, \mu_{s0})$  for the number of scattering events  $k$  undergone by the received photons with pathlength  $\ell = \nu t$  is known,<sup>5</sup> being  $\nu$  the speed of light in the medium:

$$TPSF(\mu_s, t) = TPSF(\mu_{s0}, t) \sum_{k=0}^{\infty} p_\ell(k, \mu_{s0}) \left( \frac{\mu_s}{\mu_{s0}} \right)^k e^{-(\mu_s - \mu_{s0})\ell}, \quad (1)$$

In particular, in the case of an infinite non-absorbing homogeneous medium, the function  $p_\ell(k, \mu_{s0})$  can be explicitly calculated: resulting a Poisson distribution with mean value  $\bar{k}_\infty = \mu_{s0}\ell$ :<sup>5</sup>

$$p_{\ell, \infty}(k, \mu_{s0}) = \frac{(\mu_{s0}\ell)^k}{k!} e^{-\bar{k}_\infty}, \quad (2)$$

In the case of finite geometries, instead, the probability function  $p_\ell(k, \mu_{s0})$  has to be reconstructed by using MC simulations, where for each photon received is recorded not only the trajectory length  $\ell$ , but also the number of scattering events  $k$  it underwent. Some examples of these distributions, that we named  $p_{\ell, MC}(k, \mu_{s0})$ , are reported in Fig. 1 for a non-absorbing homogeneous cylinder and for reflectance geometry (where the source and detectors belong to the upper face of the cylinder), considering different source-detector separations. In Fig. 1 also the corresponding functions  $p_{\ell, \infty}(k)$  are reported as a reference. We explicitly note that in plots of Fig. 1 they are not reported lines for those values of  $\rho$  that are greater than  $\ell$ : as a matter of fact,  $p_{\ell, MC}(k)$  is not defined when  $\rho > \ell$  because no photon can reach the detector in this case.

By inspecting Fig. 1, we can note that the distributions  $p_{\ell, MC}(k, \mu_{s0})$  tend to the corresponding  $p_{\ell, \infty}(k, \mu_{s0})$  as long as the pathlength  $\ell$  increases, in particular becoming larger and larger than source-detector distance  $\rho$ . Only when  $\ell \gtrsim \rho$  the  $p_{\ell, MC}(k, \mu_{s0})$  differ appreciably from the corresponding  $p_{\ell, \infty}(k, \mu_{s0})$ . In the latter case, differences seem mainly due to a shift in the peak position of the curves, that is moved towards smaller values of  $k$  for  $p_{\ell, MC}(k, \mu_{s0})$  with respect to the  $p_{\ell, \infty}(k, \mu_{s0})$ . Instead, the shape of  $p_{\ell, MC}(k, \mu_{s0})$  results quite similar to those of  $p_{\ell, \infty}(k, \mu_{s0})$ , *i.e.* to Poisson distributions. Finally, we note that the results reported in Fig. 1 are relative to a diffusive medium with the anisotropy factor  $g = 0$ , but similar findings and observations can be done for anisotropic scattering functions with  $g = 0.8$  (data not shown).<sup>6</sup>

Taking into account these considerations, in order to describe analytically the probability functions  $p_{\ell, MC}(k, \mu_{s0})$ , we argue that they are still Poisson distributions, as in the infinite non-absorbing homogeneous medium, but with the mean value given by the average  $\bar{k}$  of the scattering events  $k$  of each received photon. We named these Poisson distributions  $p_{\ell, a}(k, \mu_{s0})$ :

$$p_{\ell, a}(k, \mu_{s0}) = \frac{(\bar{k})^k}{k!} e^{-\bar{k}}, \quad (3)$$

where  $\bar{k}$  is calculated considering the number of scattering events  $k$  of all the received photons that traveled the same pathlength  $\ell$ . In general,  $\bar{k}$  depends on the geometry, the pathlength  $\ell$ , the scattering coefficient  $\mu_{s0}$  and the source-detector distance  $\rho$ .

In Fig. 2, we compare the probability functions  $p_{\ell, MC}(k, \mu_{s0})$  already reported in Fig. 1 with the Poisson distributions calculated according to Eq. (3). From this figure one can see that the distributions functions  $p_{\ell, MC}(k, \mu_{s0})$  are very well approximated by the Poisson distributions  $p_{\ell, a}(k, \mu_{s0})$ .

### 3. APPLICATION OF SCALING RELATIONS IN FINITE GEOMETRIES

In the previous section we found that, in the case of finite geometries, the Poisson distributions  $p_{\ell, a}(k, \mu_{s0})$  are a good approximation for the probability functions  $p_{\ell, MC}(k, \mu_{s0})$  and, then, for the functions  $p_\ell(k, \mu_{s0})$  present in Eq. (1). The knowledge of an analytical expression for the latter distributions allows applying Eq. (1) to scale an initial  $TPSF(\mu_{s0}, t)$  when a different scattering coefficient is considered. In particular, by inserting Eq. (3) into Eq. (1), it is possible to calculate an explicit expression for the scattering scaling factor  $F_s$  for  $TPSF(\mu_s, t)$ :

$$\begin{aligned} F_s &= \frac{TPSF(\mu_s, t)}{TPSF(\mu_{s0}, t)} = e^{-(\mu_s - \mu_{s0})\ell} \sum_{k=0}^{\infty} \frac{(\bar{k})^k}{k!} e^{-\bar{k}} \left( \frac{\mu_s}{\mu_{s0}} \right)^k = e^{-(\mu_s - \mu_{s0})\ell - \bar{k}} \sum_{k=0}^{\infty} \frac{1}{k!} \left( \bar{k} \frac{\mu_s}{\mu_{s0}} \right)^k = e^{-(\mu_s - \mu_{s0})\ell - \bar{k}} e^{\bar{k}\mu_s/\mu_{s0}} = \\ &= e^{-(\mu_s - \mu_{s0})\ell - (1 - \mu_s/\mu_{s0})\bar{k}} = e^{(1 - \mu_s/\mu_{s0})\mu_{s0}\ell - (1 - \mu_s/\mu_{s0})\bar{k}} = e^{k_\infty(1 - \mu_s/\mu_{s0})(1 - \bar{k}/k_\infty)}. \end{aligned} \quad (4)$$

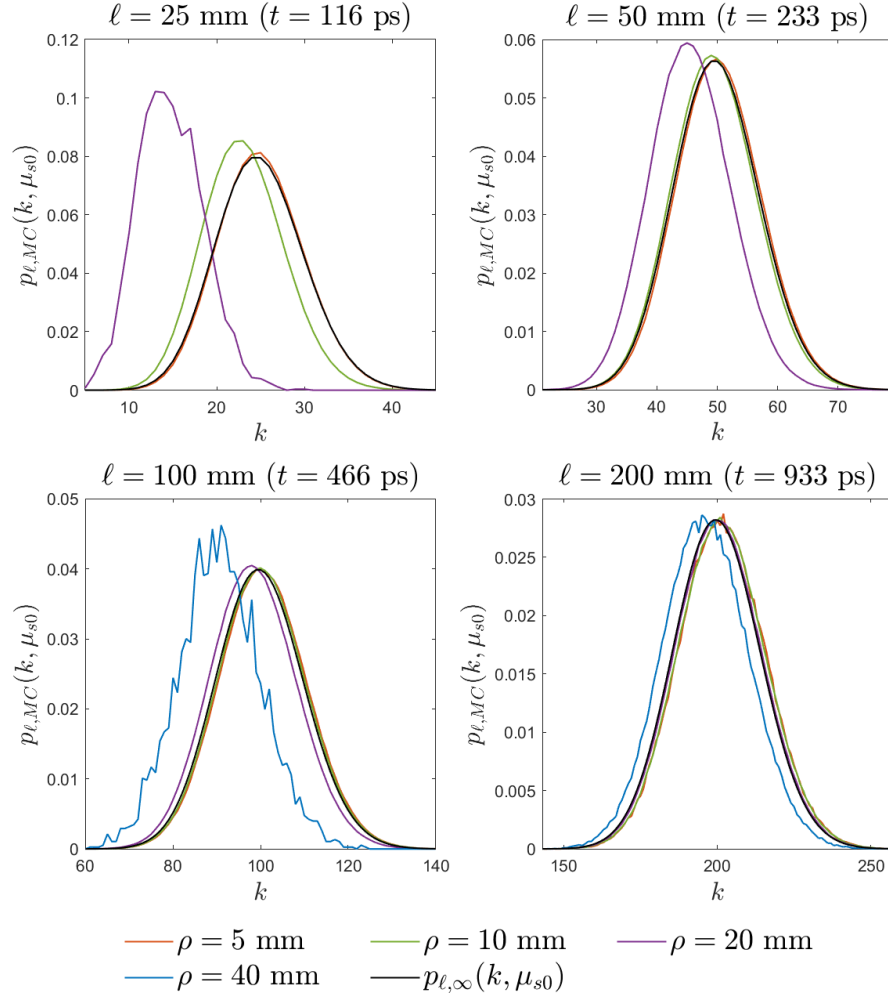


Figure 1. Examples of probability functions  $p_{\ell,MC}(k, \mu_{s0})$  for different pathlengths  $\ell$ , *i.e.* different arrival times  $t = \ell/v$ , being  $v$  the speed of light in the medium, are reported for a non-absorbing homogeneous cylinder with radius 50 mm, thickness 10 mm, reduced scattering coefficient  $\mu'_{s0} = \mu_{s0}(1 - g) = 1 \text{ mm}^{-1}$ , anisotropy factor  $g = 0$ , refractive index  $n = 1.4$ . For each  $\ell$  different source-detector distances  $\rho$  are considered. As a reference, the corresponding function  $p_{\ell,\infty}(k, \mu_{s0})$  is also reported in each plot.

Figure 3 compares the *TPSF* obtained with Eq. (1), referred to as “scaled *TPSF*”, and the direct MC simulations, referred to as “direct *TPSF*”, in the case of a homogeneous cylinder with radius 50 mm, thickness 10 mm, for 3 source-detector distances in reflectance geometry:  $\rho = 10, 20, 30$  mm. Moreover, we assumed an anisotropy factor of the medium  $g = 0$  and a refractive index  $n = 1.4$ . In particular, in Fig. 3 we report results for different scaling factors of the reduced scattering coefficient  $\mu'_s = \mu_s(1 - g)$  starting from an initial MC simulation performed with  $\mu'_{s0} = 1 \text{ mm}^{-1}$ : in the first, second and third row we applied a scaling of 10%, 50% and -50% to the reduced scattering coefficient, respectively. Again, similar findings can be found for  $g = 0.8$  (data not shown).

From Fig. 3 we can observe that also for the largest considered variations of  $\mu'_s$  the scaled *TPSF* are reasonably close to the direct ones, the deviations being  $\lesssim 50\%$  and occurring for late arrival times.<sup>6</sup>

#### 4. DISCUSSION AND CONCLUSIONS

In this work we focused on the feasibility of using SR for scattering coefficient to scale MC simulations. It results that for scaling the scattering coefficient of a *TPSF* from an initial value  $\mu_{s0}$  to a new value  $\mu_s$  the probability function  $p_{\ell}(k, \mu_{s0})$  for the number of scattering events  $k$  undergone by the received photons in the initial MC simulation is needed. To

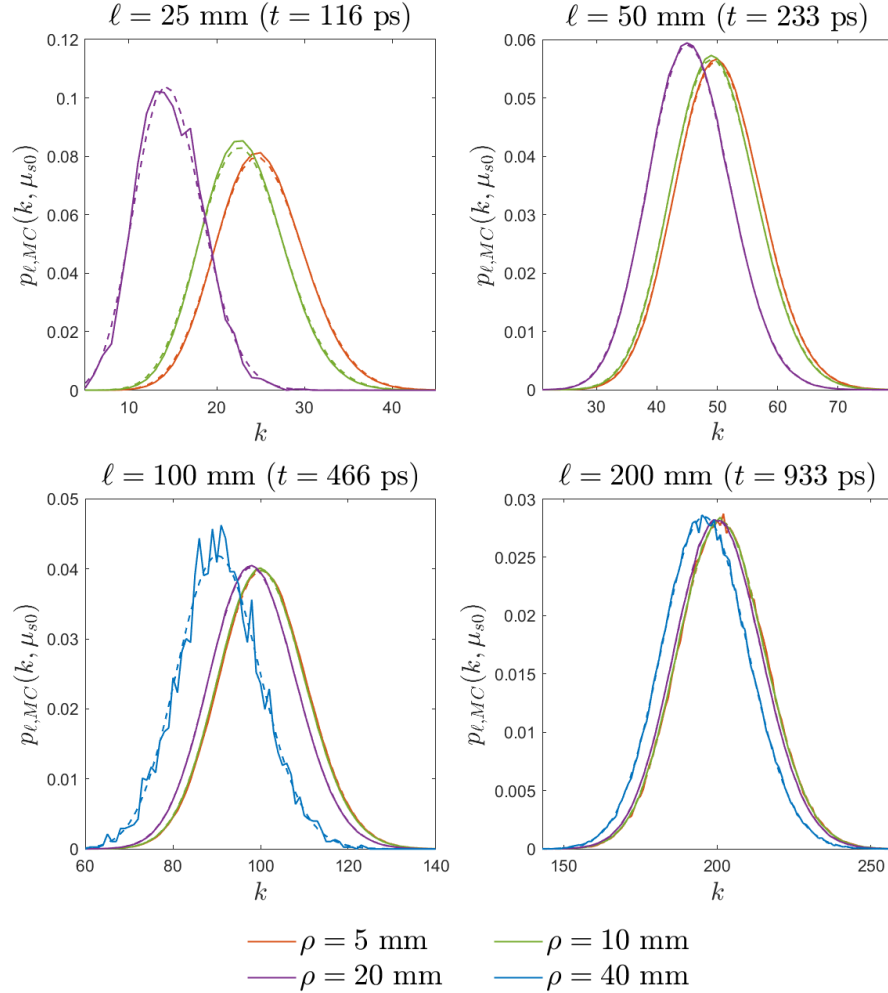


Figure 2. The same distribution functions  $p_{\ell, MC}(k, \mu_{s0})$  (solid lines) reported in Fig. 1 are here compared with the Poisson distributions  $p_{\ell, a}(k, \mu_{s0})$  (dashed lines) calculated according to Eq. (3).

this extent, as first result, we observed that distributions  $p_{\ell}(k, \mu_{s0})$  can be well approximated by Poisson distributions with mean value given by the average  $\bar{k}$  of the scattering events  $k$  of received photons in the initial simulation (*i.e.*  $\mu_s = \mu_{s0}$ ). Then, we compared the scaled *TPSF*, calculated by using this method, with the exact MC simulations for some geometrical and optical parameters, obtaining satisfactory results: in particular, this approach causes deviations of scaled *TPSF* that occur for late arrival times and are  $\lesssim 50\%$  for variations of the reduced scattering coefficient up to  $\pm 50\%$ . As a general remark, the use of  $p_{\ell, a}(k, \mu_{s0})$  promises to improve the convergence properties of SR for the scattering coefficient, overcoming the under-sampling problems shown in Ref. 6.

### ACKNOWLEDGMENTS

This study was partially supported and funded by the following Projects:

- MUR-PRIN2020, Trajector-AGE, grant number: 2020477RW5PRIN.
- NextGenerationEU, National Recovery and Resilience Plan, Agritech National Research Center, CN00000022 (DD 1032 17.06.2022).
- NextGenerationEU, National Recovery and Resilience Plan, MNESYS, PE0000006 (DN 1553 11.10.2022).
- NextGenerationEU, National Recovery and Resilience Plan, Age-IT, PE0000015 (DD 1557 11.10.2022).

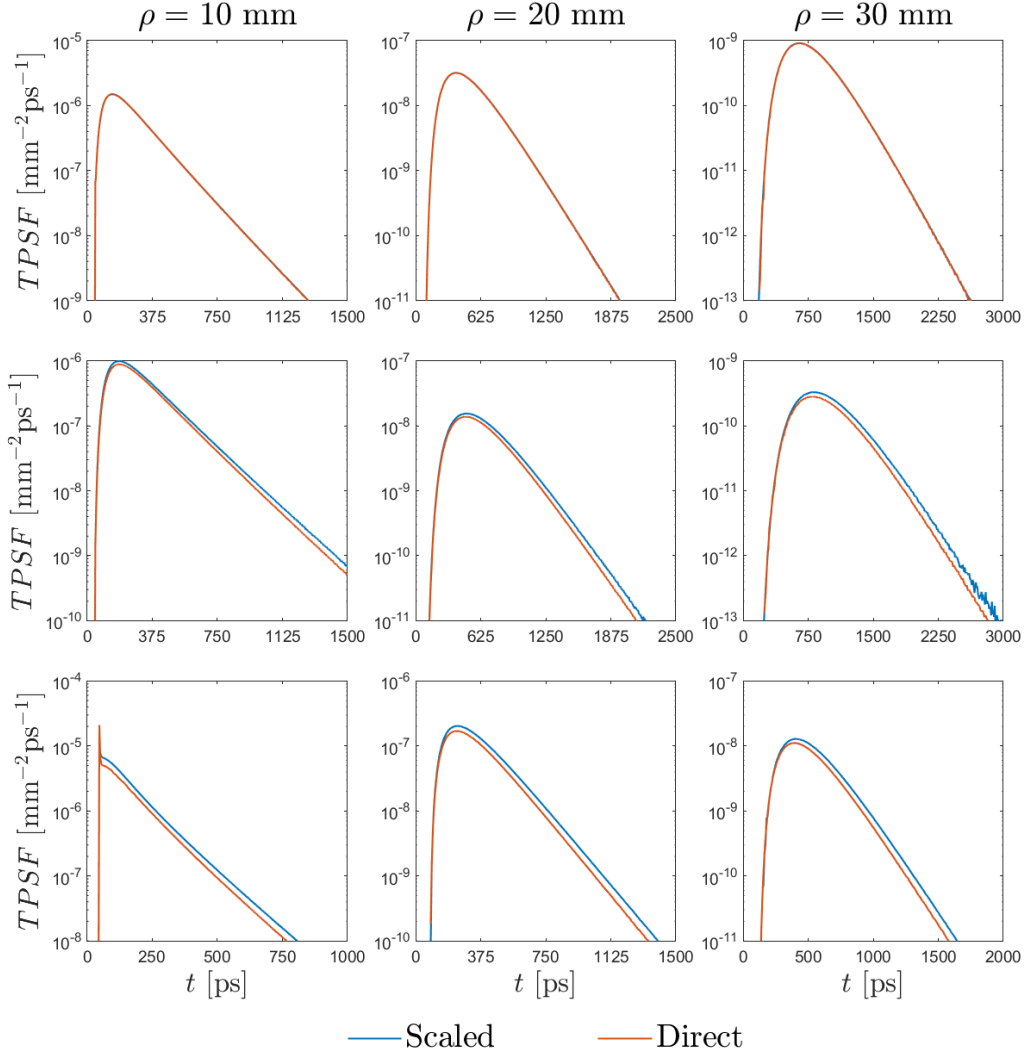


Figure 3. Comparison between  $TPSF$  as a function of time obtained by direct MC simulations and by scaling an initial MC simulation for  $\mu'_{s0} = 1 \text{ mm}^{-1}$  to:  $\mu'_s = 1.1 \text{ mm}^{-1}$  (first row);  $\mu'_s = 1.5 \text{ mm}^{-1}$  (second row);  $\mu'_s = 0.5 \text{ mm}^{-1}$  (third row). The results presented are relative to a homogeneous cylinder with radius 50 mm, thickness 10 mm, refractive index  $n = 1.4$ ,  $g = 0$ , considering three source-detector distances:  $\rho = 10 \text{ mm}$  (first column);  $\rho = 20 \text{ mm}$  (second column);  $\rho = 30 \text{ mm}$  (third column). Scaled  $TPSF$  are obtained with about  $N \approx 10^9$  detected photons.

- NextGenerationEU, National Recovery and Resilience Plan, PRIN 2022, grant number: 20227EPKW2.
- NextGenerationEU, National Recovery and Resilience Plan, PRIN 2022, DIRS, grant number: 2022EB4B7E.
- National Institutes of Health: R01-EB029414.
- Horizon 2020 Framework Programme of the European Union (grant agreement number 863087).
- European Innovation Council under the Pathfinder Open call (grant agreement number 101099093).

## REFERENCES

- [1] Fang, Q. and Boas, D. A., “Monte Carlo simulation of photon migration in 3d turbid media accelerated by Graphics Processing Units,” *Opt. Express* **17**, 20178–20190 (Oct 2009).
- [2] Yan, S. and Fang, Q., “Hybrid mesh and voxel based Monte Carlo algorithm for accurate and efficient photon transport modeling in complex bio-tissues,” *Biomed. Opt. Express* **11**, 6262–6270 (Nov 2020).

- [3] Sassaroli, A., Blumetti, C., Martelli, F., Alianelli, L., Contini, D., Ismaelli, A., and Zaccanti, G., "Monte Carlo procedure for investigating light propagation and imaging of highly scattering media," *Applied Optics* **37**, 7392–7400 (11 1998).
- [4] Yao, R., Intes, X., and Fang, Q., "Direct approach to compute Jacobians for diffuse optical tomography using perturbation Monte Carlo-based photon replay," *Biomedical Optics Express* **9**, 4588–4603 (10 2018).
- [5] Amendola, C., Maffeis, G., Farina, A., Spinelli, L., Torricelli, A., Pifferi, A., Sassaroli, A., Fanelli, D., Tommasi, F., and Martelli, F., "Application limits of the scaling relations for Monte Carlo simulations in diffuse optics. Part 1: theory," *Opt. Express* **32**, 125–150 (Jan 2024).
- [6] Amendola, C., Maffeis, G., Farina, A., Spinelli, L., Torricelli, A., Pifferi, A., Sassaroli, A., Fanelli, D., Tommasi, F., and Martelli, F., "Application limits of the scaling relations for Monte Carlo simulations in diffuse optics. Part 2: results," *Opt. Express* **32**, 26667–26689 (Jul 2024).